IDLE MOTION DURING PROPULSION OF WHEELCHAIRS WITH DRIVETRAIN SYSTEMS EQUIPPED WITH TRANSMISSIONS

Lukasz Wargula, Mateusz Kukla
Poznan University of Technology, Poland
lukasz.wargula@put.poznan.pl, mateusz.kukla@put.poznan.pl

Abstract. This article presents a study of six wheelchairs: a classic push-rim manual wheelchair (A), a hybrid electric-manual wheelchair (manual variant powered by a push rim) (B), a wheelchair with a geared planetary transmission (C), a wheelchair with a belt variator transmission (D), a wheelchair with a planetary transmission regulating the gear ratio combined with a chain drive (adapted from bicycle applications) (E), and a wheelchair with a chain transmission regulating the gear ratio combined with a chain drive (adapted from bicycle applications) (F). The propulsion mechanisms, particularly the transmissions, are characterized by backlash, which results in idle motion during the propulsion stroke. The study measured the angular range of idle motion, based on which the percentage range of idle motion of the wheelchair user's limb during a single propulsion stroke was determined. It was shown that wheelchairs A and B exhibit no backlash, whereas the idle motion angle and percentage range of idle motion per stroke were as follows: for C, depending on the gear ratio – reducer 43.5° and 72.5%, 1:1 ratio 0° and 0%, multiplier 11° and 18.3%; for E, 9.7° and 16.1%; and for F, 7.5° and 12.5%; for construction D, 26° and 43%. The percentage of idle motion was calculated by subtracting the measured angular motion range from the assumed total motion range (set at 60°), corresponding to the technique of gentle pushes at low speeds. Additionally, the maneuverability of the wheelchair was analyzed by measuring the backlash during push-rim movement in reverse. It was found that constructions A and B had no backlash, C – depending on the gear ratio: reducer 91°, 1:1 ratio 52°, multiplier 74°, D had 26° (same as forward), E had 66° and F exhibited no reverse movement (no maneuverability in reverse).

Keywords: assistive technology, wheelchair, propelled wheelchair, disabled transport.

Introduction

Hand movement during manual wheelchair propulsion is a complex process influenced by various biomechanical factors, including hand pressure, grip force, propulsion techniques, and mechanical efficiency. During propulsion, hand pressure on the palm typically ranges from 180 to 200 kPa, with shoulder and elbow joint movements varying between 30° to 70° and 15° to 50°, respectively [1]. Grip force is affected by wheelchair design, with models like the Action3 generating higher grip forces than the Neater Uni-wheelchair, potentially increasing the risk of repetitive strain injuries [2]. Different propulsion techniques involve four distinct hand patterns – arc, single loop, double loop, and semicircular – the latter being biomechanically advantageous, though the double loop pattern minimizes muscle stress and power demands [3]. Stroke patterns, such as pumping, semicircular, and single-looping, also impact efficiency, with pumping being the most effective [4]. Biomechanical efficiency is enhanced through controlled bimanual force application, with initial learning stages characterized by a shift from high-frequency movements to longer, slower strokes with reduced power loss [5]. Energy models based on physiological and biomechanical principles aid in optimizing propulsion efficiency and reducing joint strain [6]. Additionally, innovative propulsion systems, including lever-driven wheelchairs and rowing-inspired motion, offer potential improvements in movement efficiency and injury prevention [7; 8]. The distribution of mass within the wheelchair affects propulsion forces, with rear-wheel or footrest placements increasing the required force [9]. Ergonomic handrims, such as the Natural-Fit, help reduce grip strain and discomfort, while shoulder pain is linked to changes in propulsion biomechanics, highlighting the importance of optimizing propulsion strategies [10; 11]. Understanding these factors is essential for designing wheelchairs that enhance both performance and user comfort.

Wheelchair propulsion assistance systems incorporate various mechanical designs to enhance mobility and reduce user strain. Ratchet systems enable forward propulsion without backward movement when resetting the levers, offering a universally adaptable solution for different wheelchair types [12]. Lever propulsion with variable gear ratios can significantly reduce shoulder joint contact forces, with a 1/1.5 gear ratio lowering force by up to 70% compared to handrim propulsion [13]. Optimizing lever length and rotation axis relative to the user' s shoulder further improves movement efficiency [7]. Chain transmission systems, akin to bicycle mechanisms, provide variable gear ratios between the wheels and pushrims, allowing users to adjust driving torque based on physical capabilities

and terrain conditions. Planetary gear systems dynamically modify torque demands, aiding movement on soft surfaces or inclines, while multi-functional planetary gears can enhance stair-climbing wheelchairs by improving stability and safety [14]. Motor-assisted propulsion integrates powered drive wheels to minimize initial force requirements, shorten stopping distances, and reduce physical exertion [15]. Advanced control signals based on muscle activity can regulate gear ratios or supplementary propulsion, creating a system that adapts to the user's physical input for greater efficiency and comfort [16; 17]. The potential for additional drive mechanisms in wheelchair designs to introduce idle movement, thereby increasing the proportion of idle work during propulsion, is a critical consideration in mobility optimization. Propulsion efficiency may be affected by innovative systems like active-caster drives, which enable independent control of translational and rotational motions but add complexity [18; 19]. Geared manual wheelchair wheels, though designed to reduce upper extremity strain, require more stroke cycles for the same distance, potentially increasing idle movement [20]. Energy cost and mechanical efficiency in manual propulsion are already low, as a significant portion of applied forces does not contribute to forward motion, and improperly integrated assistive technologies may further reduce efficiency [21; 22]. Weight distribution is another crucial factor, as imbalances can raise propulsion forces and idle work [23]. Mechanical and kinetic considerations, including the positioning of additional drive mechanisms, influence propulsion dynamics, with misalignment potentially increasing rolling resistance and unnecessary movement [24]. In conclusion, while additional drive systems can offer benefits, their impact on propulsion efficiency must be carefully managed through proper design, weight distribution, and system optimization to minimize idle work and enhance mobility performance.

The article presents research on the impact of various wheelchair designs developed at the Poznań University of Technology, including a hybrid electric-manual wheelchair, a wheelchair with a planetary gear system, a chain-driven wheelchair (adapted from bicycle mechanisms), a belt-driven transmission, and traditional push-rim-propelled wheelchairs. The study focuses on the effect of these designs on idle limb movement, which refers to motion that does not contribute to wheelchair propulsion but rather compensates for idle displacement within the transmission systems. The aim of the study is to examine the contribution of upper limb idling motion during the propulsion of wheelchairs equipped with innovative structural solutions. These design features – while often overlooked during the planning of assistive drive systems – may be considered a drawback, as they can limit propulsion efficiency and maneuverability.

Materials and methods

Six wheelchairs were analyzed in the study: a classic push-rim-propelled wheelchair (A) [25] (Fig. 1), a hybrid electric-manual wheelchair (B) [26; 27] (manual variant powered by push rims) (Fig. 2), a planetary gear wheelchair with a geared transmission (C) [28] (Fig. 3), a belt-driven continuously variable transmission (CVT) wheelchair using a V-belt (D) (Fig. 4), a planetary gear wheelchair with adjustable gearing combined with a chain drive (adapted from bicycle applications) (E) (Fig. 5), and a chain-driven wheelchair with adjustable gearing (also adapted from bicycle applications) (F) (Fig. 6).

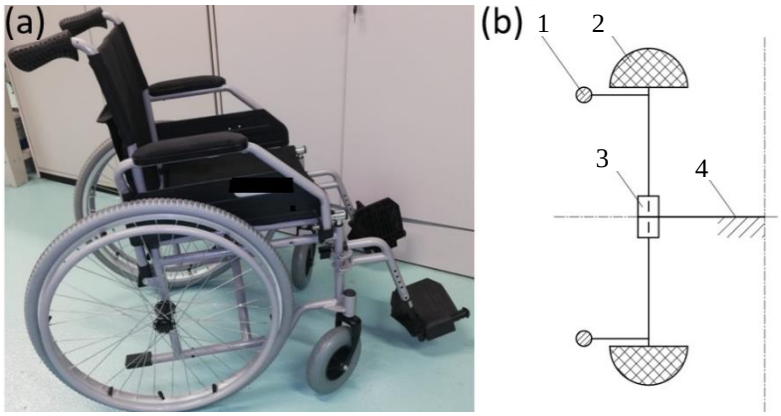

Fig. 1. **Classic push-rim manual wheelchair (A):** a – physical model; b – kinematic diagram of a single-wheel drive system; 1 – push-rim; 2 – tire; 3 – radial ball bearing; 4 – wheelchair frame

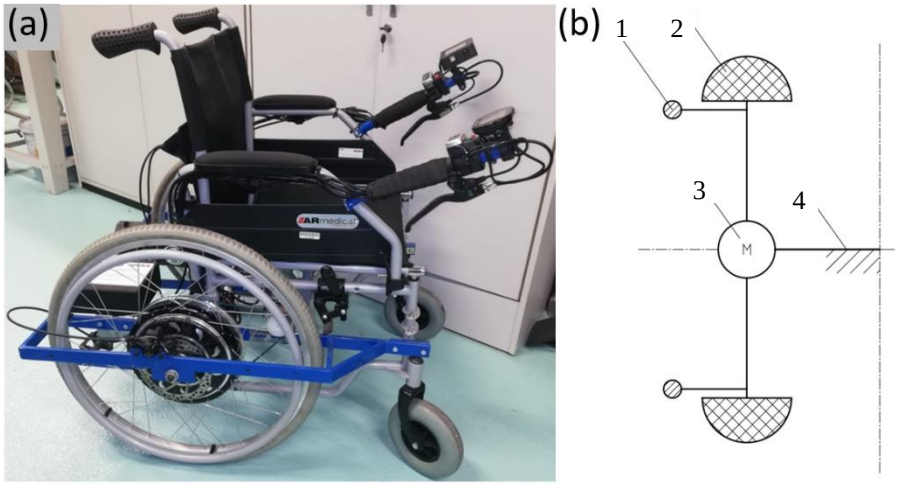

Fig. 2. **Hybrid electric-manual wheelchair (manual variant powered by a push-rim) (B):** a – physical model; b – kinematic diagram of the single-wheel drive system; 1 – push-rim; 2 – tire; 3 – BLDC motor; 4 – wheelchair frame

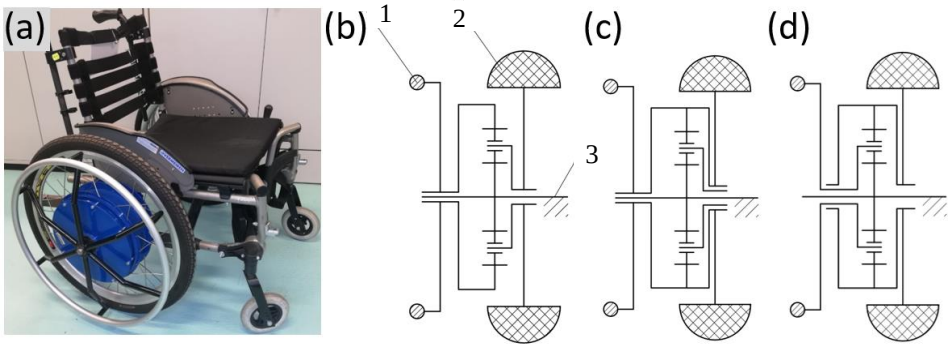

Fig. 3. **Wheelchair with a geared planetary transmission (C):** a – physical model; b – kinematic diagram of the single-wheel drive system in the multiplier configuration; c – kinematic diagram of the single-wheel drive system in the neutral configuration; d – kinematic diagram of the single-wheel drive system in the reducer configuration; 1 – push-rim; 2 – tire; 3 – wheelchair frame

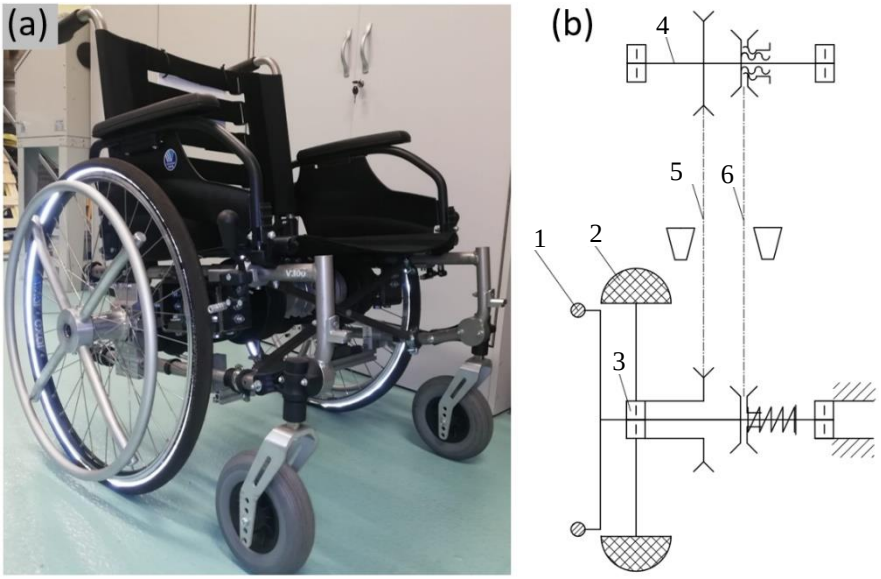

Fig. 4. **Wheelchair with a belt variator transmission (D):** a – physical model; b – kinematic diagram of the single-wheel drive system; 1 – push-rim; 2 – tire; 3 – radial ball bearing; 4 – intermediate shaft; 5 – belt transmission with a V-belt (1:1 ratio); 6 – variator belt transmission with ratio adjustment via control knob

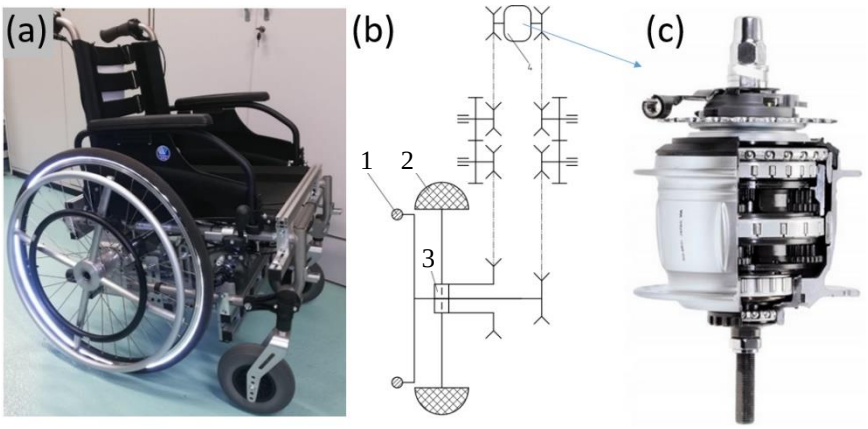

Fig. 5. **Wheelchair with a planetary gear and an adjustable transmission, combined with a chain drive (adapted from bicycle applications) (E):** a – physical model; b – kinematic diagram of the single-wheel drive system; 1 – push-rim; 2 – tire; 3 – wheelchair frame; 4 – bicycle planetary gear; c – model of a bicycle planetary gear "Shimano Nexus 7"

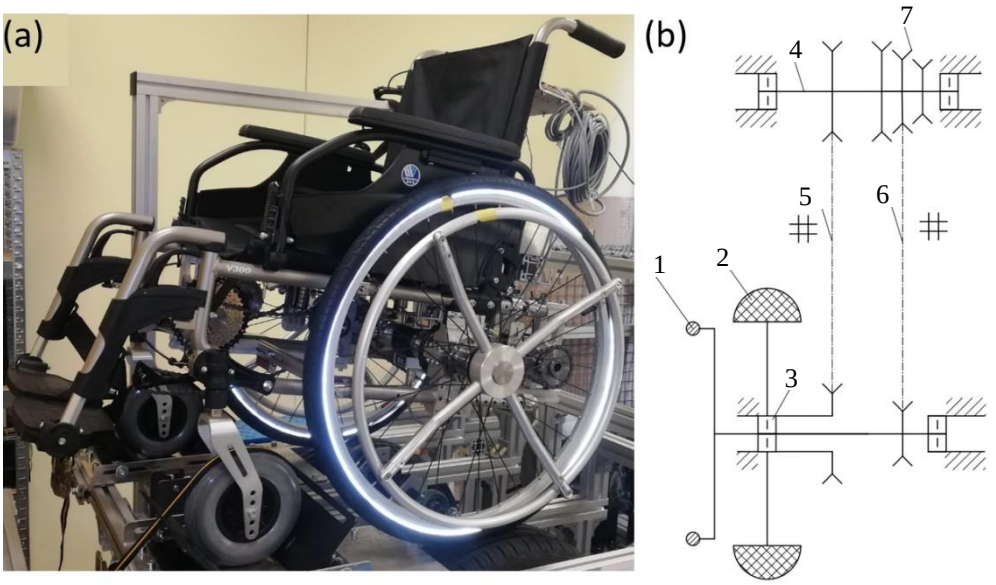

Fig. 6. **Chain-driven wheelchair with adjustable gearing (adapted from bicycle applications) (F):** a – physical model; b – kinematic diagram of the single-wheel drive system; 1 – push-rim; 2 – tire; 3 – radial ball bearing; 4 – intermediate shaft; 5 – chain; 6 – chain; 7 – stepped chain transmission

A detailed description of the tested designs is provided in the attached literature list. The general characteristics indicate that for push-rim propulsion, the push rims had a diameter of 53 mm, and the main wheels were 24 inches. Wheelchair B featured a hub motor with a BLDC electric motor adapted from bicycle applications, where the rim and push rims were attached via spokes. Wheelchair C was equipped with a planetary gear system in the wheel hubs, offering a 1:1 gear ratio, a reduction to 0.51, or multiplication to 1.96. In the 1:1 setting, the wheelchair exhibited no backlash between the gears. Wheelchairs D, E, and F utilized a hub that enabled power transfer from the push rims through a transmission system to the drive wheels. Wheelchair D used a belt-driven CVT, while wheelchairs E and F incorporated adaptations of multi-speed bicycle mechanisms: wheelchair E featured a multi-speed hub, whereas wheelchair F used a stepped chain transmission. Constructions from B-F are original constructions of authors from the Poznań University of Technology, the details of which can also be found in the Polish Patent Office.

The study measured the angular range of idle motion, based on which the percentage range of idle motion of the wheelchair user's limb during a single propulsion stroke was determined. The percentage of idle motion was calculated by subtracting the measured angular motion range from the assumed total motion range (set at 60° [29]), corresponding to the technique of gentle pushes at low speeds.

Additionally, the manoeuvrability of the wheelchair was analyzed by measuring the backlash during push-rim movement in reverse (Fig. 7 and 8). The angular value θ was determined during the experiments based on the measured arc length s along the push-rim diameter r, in accordance with Equation (1). The measurement was carried out using a Class I accuracy tape measure (precision ± 0.1 mm).

$$\theta = \frac{s}{r} \cdot \frac{180^{\circ}}{\pi}. \quad (1)$$

For the statistical analysis of the angular test results, the Student's t-distribution was used, based on which the confidence interval was determined for the probability level $p = 0.05$.

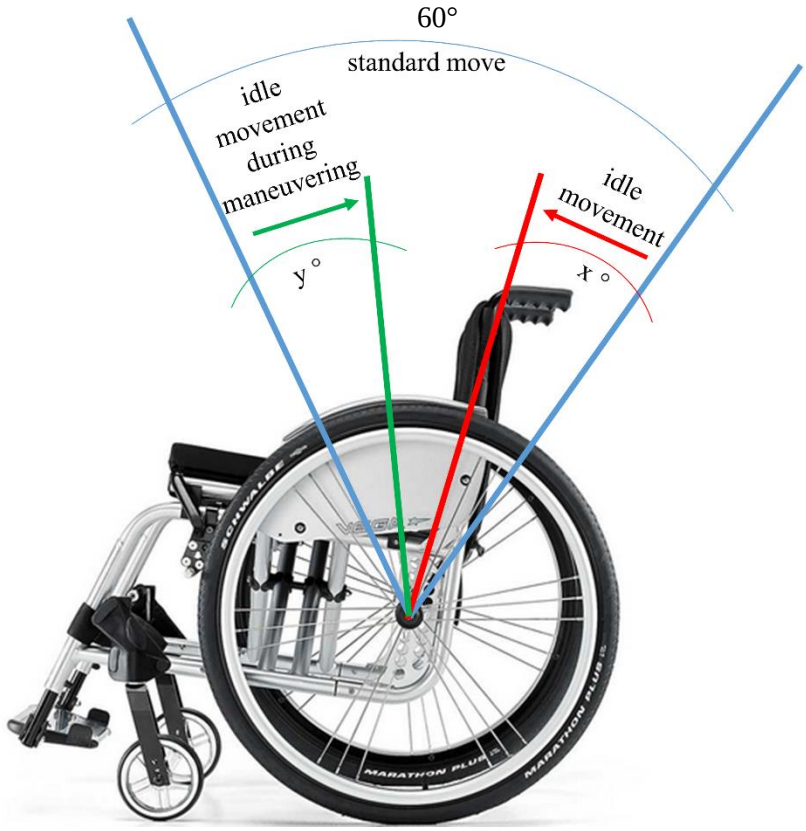

Fig. 7. **Movement of the limb while propelling the wheelchair using a push rim:** blue – 100% movement; red – idle movement during propulsion; green – idle movement during maneuvering; x – idle angle during propulsion; y – idle angle during maneuvering

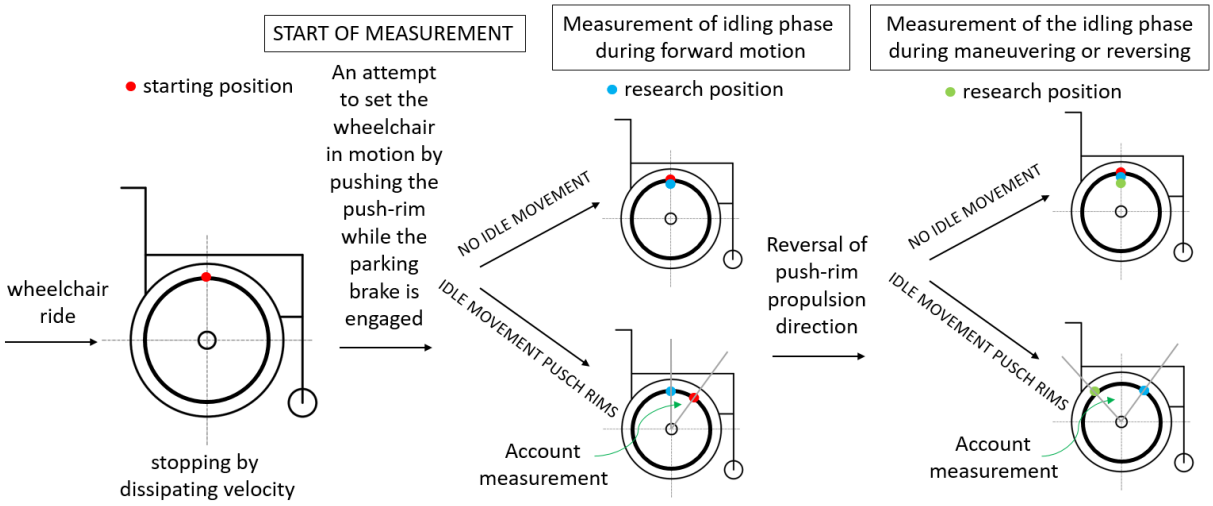

Fig. 8. **Schematic representation of the measurement procedure**

Results and discussion

The results of the angular measurement during wheelchair propulsion and maneuvering are presented in Table 1. The idle motion values during propulsion, depending on the wheelchair design, are shown in Fig. 9. Wheelchairs A and B (traditional push-rim and hybrid electric-manual in manual mode) exhibited no measurable idle motion, demonstrating direct force transmission without backlash. This is expected, as these designs do not include additional gearing systems that could introduce mechanical play.

Table 1

Angle measurement test results

Construction – variant	***x*** **– idle angle during propulsion**	***p*** **= 0.05**	***y*** **– idle angle during maneuvering**	***p*** **= 0.05**
A	no backlash	-	no backlash	-
B	no backlash	-	no backlash	-
C – reducer	43.5 °	± 1.5 °	91 °	± 2.2 °
C – 1:1 ratio	no backlash	-	no backlash	-
C – multiplier	11°	± 0.5 °	74 °	± 2.1 °
D (gear ratio did not affect the number of cooperating components)	26 °	± 0.8 °	26 °	± 0.8 °
E (gear ratio did not affect the number of cooperating components)	9.7 °	± 0.4 °	66 °	± 2 °
F (gear ratio did not affect the number of cooperating components)	7.5 °	± 0.4 °	no maneuverability in reverse	-

In contrast, wheelchair C with a reducer (C – reducer) showed the highest idle angle during both propulsion (43.5° ± 1.5°) and maneuvering (91° ± 2.2°). This significant idle movement suggests that the reducer introduces a considerable amount of mechanical backlash, which could reduce propulsion efficiency and maneuverability. However, when the same planetary gear system was used at a 1:1 ratio (C – 1:1 ratio), no idle motion was observed, indicating that the backlash issue is specific to the reduction mechanism rather than the planetary gear system itself. Conversely, in C – multiplier mode, where the transmission increases speed, the idle angle was significantly reduced to 11° ± 0.5° during propulsion and 74° ± 2.1° during maneuvering. This suggests that while the multiplier introduces some idle motion, it is far less than the reducer, possibly due to the way mechanical engagement occurs in higher-speed gearing.

For wheelchairs D, E, and F, all of which incorporate alternative transmission mechanisms, the results reveal varying levels of idle motion. Wheelchair D (belt-driven continuously variable transmission – CVT) exhibited an idle angle of 26° ± 0.8° during both propulsion and maneuvering, indicating a moderate level of mechanical play, likely due to the nature of belt-driven power transfer. Wheelchair E, featuring a multi-speed planetary gear hub, performed better with an idle motion of 9.7° ± 0.4° during propulsion and 66° ± 2° during maneuvering, suggesting that the integration of planetary gearing with a chain drive effectively reduces idle motion compared to purely belt-driven solutions. Wheelchair F, utilizing a stepped chain transmission, showed the lowest idle motion among geared wheelchairs, with only 7.5° ± 0.4° during propulsion. However, it was unable to perform reverse maneuvers, implying that the chain-driven gearing system does not allow for efficient bidirectional movement.

The findings suggest that direct-drive manual wheelchairs (A and B) offer the highest propulsion efficiency, as they completely eliminate idle motion. However, these designs lack the mechanical advantage of gearing systems, which can reduce the physical strain on users. In contrast, wheelchairs with planetary reducers (C – reducer) introduce significant idle movement, which may negatively impact propulsion efficiency, requiring additional effort to compensate for lost motion. On the other hand, the planetary multiplier (C – multiplier) significantly reduces idle movement compared to the reducer, making it a more efficient gearing solution.

Among alternative drive mechanisms, belt-driven systems (D) showed moderate idle motion, while multi-speed planetary hubs (E) and stepped chain transmissions (F) provided the lowest idle motion, making them more effective at maintaining efficiency. However, the lack of reverse maneuverability in wheelchair F is a notable limitation, restricting its usability in confined spaces where backward adjustments are necessary.

Overall, the study highlights a trade-off between mechanical gearing advantages and idle motion efficiency. While gearing systems can assist users by reducing physical strain, improper selection or design can introduce excessive idle motion, diminishing propulsion effectiveness. Future developments should focus on optimizing gear engagement mechanisms to minimize backlash while maintaining the benefits of assisted propulsion.

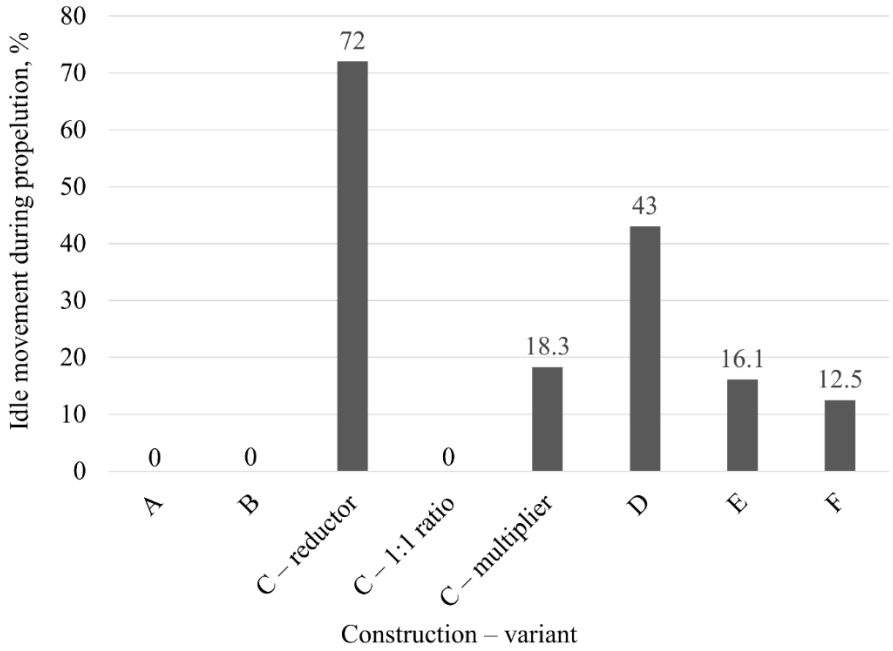

Fig. 9. **Idle movement during propulsion**

When designing wheelchairs, as well as other muscle-powered machines and devices, it is essential to consider not only energy efficiency [30], mass, ergonomics, musculoskeletal strain [31], and safety [32] but, most importantly, functionality and user comfort. Devices that are uncomfortable or limit functionality are unlikely to be widely adopted by users. It appears that due to the reduction of idle limb movement during propulsion, further development of designs A and B is beneficial. Design C is only advantageous at a 1:1 ratio, which is equivalent to propulsion without a transmission, making this solution impractical as well. For planetary gear-driven systems, it is important to explore new design solutions [33], such as backlash-free planetary gears, which eliminate or minimize gear backlash.

Conclusions

1. Constructions A, B, and C (in the 1:1 gear ratio position), which directly transmit the driving torque from the push-rim to the wheel rim, are characterized by high efficiency due to the absence of idling motion during wheelchair propulsion.
2. Gear backlash must be considered during design, as it can significantly impact propulsion efficiency and maneuverability in wheelchairs.
3. Hybrid electric-manual drives with hub motors do not introduce idle motion, just like traditional push-rim propulsion systems.
4. The use of mechanical transmissions can lead to 12.5% to 72% idle motion during wheelchair propulsion, reducing efficiency.
5. The angular motion required to overcome gear backlash or transmission tension (belt or chain) during wheelchair propulsion can range from 7.5° to 43°.
6. The angular motion required to overcome gear backlash or transmission tension during wheelchair maneuvering can range from 26° to 91°.

Funding

This research is a part of the project: "Innovative Drive Systems for Wheelchairs – Design, Prototype, Research, number: "Rzeczy są dla ludzi/0004/2020" financed by National Centre for Research and Development, https://www.gov.pl/web/ncbr (accessed on: 3 October 2021).

Author contributions

Conceptualization, Ł.W. ; methodology, Ł.W., software, Ł.W. and M.K., validation, Ł.W. and M.K., formal analysis, Ł.W., investigation, Ł.W. and M.K., data curation, Ł.W., writing – original draft preparation, Ł.W. and M.K., writing – review and editing, Ł.W. and M.K., visualization, Ł.W. and M.K., project administration, Ł.W. and M.K., funding acquisition, Ł.W. and M.K. All authors have read and agreed to the published version of the manuscript.

References

[1] Kabra C., Jaiswal R., Arnold G., Abboud R., Wang W. Analysis of Hand Pressures Related to Wheelchair Rim Sizes and Upper-Limb Movement. Int. J. Ind. Ergon. 2015, 47, pp. 45-52, DOI: 10.1016/j.ergon.2015.01.015.

[2] Mandy A., Redhead L., Michaelis J. Measurement of Hand/Handrim Grip Forces in Two Different One Arm Drive Wheelchairs. BioMed Res. Int. 2014, 2014, DOI: 10.1155/2014/509898.

[3] Slowik J.S., Requejo P.S., Mulroy S.J., Neptune R.R. The Influence of Wheelchair Propulsion Hand Pattern on Upper Extremity Muscle Power and Stress. J. Biomech. 2016, 49, pp. 1554-1561, DOI: 10.1016/j.jbiomech.2016.03.031.

[4] De Groot S., Veeger H.E.J., Hollander A.P., Van Der Woude L.H.V. Effect of Wheelchair Stroke Pattern on Mechanical Efficiency. Am. J. Phys. Med. Rehabil. 2004, 83, pp. 640-649, DOI: 10.1097/01.PHM.0000133437.58810.C6.

[5] Vegter R.J.K., De Groot S., Lamoth C.J., Veeger D.H., Van Der Woude L.H.V. Initial Skill Acquisition of Handrim Wheelchair Propulsion: A New Perspective. IEEE Trans. Neural Syst. Rehabil. Eng. 2014, 22, pp. 104-113, DOI: 10.1109/TNSRE.2013.2280301.

[6] Lin C.-J., Lin P.-C., Guo L.-Y., Su F.-C. Prediction of Applied Forces in Handrim Wheelchair Propulsion. J. Biomech. 2011, 44, pp. 455-460, DOI: 10.1016/j.jbiomech.2010.09.029.

[7] Choromanski W., Dobrzynski G., Fiok K. Optimization of Lever-Driven Wheelchairs., 2010; Vol. 31 IFMBE, pp. 671-674.

[8] Quaglia G., Bonisoli E., Cavallone P. A Proposal of Alternative Propulsion System for Manual Wheelchair. Int. J. Mech. Control 2018, 19, pp. 33-38.

[9] Alcoléa V., Medola F.O., da Silva Bertolaccini G., Sandnes, F.E. Effect of Added Mass Location on Manual Wheelchair Propulsion Forces. Adv. Intell. Syst. Comput. 2020, 1026, pp. 747-753, DOI: 10.1007/978-3-030-27928-8_114.

[10] Koontz A.M., Yang Y., Kanaly J., Cooper R.A., Boninger M.L., Koontz A.M., Yang Y., Boninger D.S., Cooper R.A., Boninger M.L., et al. Investigation of the Performance of an Ergonomic Handrim as a Pain-Relieving Intervention for Manual Wheelchair Users. Assist. Technol. 2006, 18, pp. 123-145, DOI: 10.1080/10400435.2006.10131912.

[11] Briley S.J., Vegter R.J.K., Goosey-Tolfrey V.L., Mason B.S. The Longitudinal Relationship between Shoulder Pain and Altered Wheelchair Propulsion Biomechanics of Manual Wheelchair Users. J. Biomech. 2021, 126, DOI: 10.1016/j.jbiomech.2021.110626.

[12] Harrington T., Murphy G. Lever Propulsion Design for Manual Wheelchairs., 2004; Vol. 30, pp. pp. 210-211.

[13] Sasaki M., Stefanov D., Ota Y., Miura H., Nakayama A. Shoulder Joint Contact Force during Lever-Propelled Wheelchair Propulsion. ROBOMECH J. 2015, 2, DOI: 10.1186/s40648-015-0037-8.

[14] Zhao Z. Layout Guide for Design of a Novel Wheelchairs with Circumferential Linkage Using Microsoft Word., 2021; Vol. 2113.

[15] Wong S., Mortenson B., Sawatzky B. Starting and Stopping Kinetics of a Rear Mounted Power Assist for Manual Wheelchairs. Assist. Technol. 2019, 31, pp. 77-81, DOI: 10.1080/10400435.2017.1366373.

[16] Warguła Ł., Marciniak A. The Symmetry of the Muscle Tension Signal in the Upper Limbs When Propelling a Wheelchair and Innovative Control Systems for Propulsion System Gear Ratio or Propulsion Torque: A Pilot Study. Symmetry 2022, 14, 1002-1-1002-1012.
[17] Wieczorek B., Warguła Ł., Gierz Ł., Zharkevich O., Nikonova T., Sydor M. Electromyographic Analysis of Upper Limb Muscles for Automatic Wheelchair Propulsion Control. Przegląd Elektrotechniczny 2024, 100, pp. 6-11.
[18] Munakata Y., Tanaka A., Wada M. A Five-Wheel Wheelchair with an Active-Caster Drive System., 2013.
[19] Munakata Y., Wada M. Development of an Add-on Drive Mechanism for Improving Motion Performance of a Manual Wheelchair., 2015; Vol. 2015-September, pp. 684-689.
[20] Jahanian O., Gaglio A., Cho C.C., Muqeet V., Smith R., Morrow M.M.B., Hsiao-Wecksler E.T., Slavens B.A. Hand-Rim Biomechanics during Geared Manual Wheelchair Propulsion over Different Ground Conditions in Individuals with Spinal Cord Injury. J. Biomech. 2022, 142, DOI: 10.1016/j.jbiomech.2022.111235.
[21] Aissaoui R., Gagnon D. Effect of Haptic Training During Manual Wheelchair Propulsion on Shoulder Joint Reaction Moments. Front. Rehabil. Sci. 2022, 3, DOI: 10.3389/fresc.2022.827534.
[22] Gabryelski J., Kurczewski P., Sydor M., Szperling A., Torzyński D., Zabłocki M. Development of Transport for Disabled People on the Example of Wheelchair Propulsion with Cam-Thread Drive. Energies 2021, 14, 8137, DOI: 10.3390/en14238137.
[23] Lin J.-T., Sprigle S. The Influence of Operator and Wheelchair Factors on Wheelchair Propulsion Effort. Disabil. Rehabil. Assist. Technol. 2020, 15, pp. 328-335, DOI: 10.1080/17483107.2019.1578425.
[24] Ott J., Henderson T., Wilson-Jene H., Koontz A., Pearlman J. A High Prevalence of Manual Wheelchair Rear-Wheel Misalignment Could Be Leading to Increased Risk of Repetitive Strain Injuries. Disabil. Rehabil. Assist. Technol. 2023, 18, pp. 544-552, DOI: 10.1080/17483107.2021.1890843.
[25] Wieczorek B. The Wheelchair Propulsion Wheel Rotation Angle Function Symmetry in the Propelling Phase: Motion Capture Research and a Mathematical Model. Symmetry 2022, 14, 576, DOI: 10.3390/sym14030576.
[26] Wieczorek B., Warguła Ł., Kukla M. Influence of a Hybrid Manual-Electric Wheelchair Propulsion System on the User's Muscular Effort. Acta Mech. Autom. 2023, 17, 28-34, DOI: 10.2478/ama-2023-0003.
[27] Wieczorek B., Warguła Ł., Rybarczyk D. Impact of a Hybrid Assisted Wheelchair Propulsion System on Motion Kinematics during Climbing up a Slope. Appl. Sci. 2020, 10, 1025, DOI: 10.3390/app10031025.
[28] Wieczorek B., Warguła Ł., Kostov B., Stambolov G. A Prototype of a Multi-Speed Gear Hub for Manual Wheelchairs-a Preliminary Analysis of the Dynamics of the Wheelchair's Motion and the Biomechanics of the Human Body. Mater. Mech. Eng. Technol. 2022, 2022, pp. 19-27, DOI: 10.52209/2706-977X_2022_4_19.
[29] Lee S.-Y., Kim S.-C., Lee M.-H., Yoo J.-S. Effect of the Height of a Wheelchair on the Shoulder and Forearm Muscular Activation during Wheelchair Propulsion. J. Phys. Ther. Sci. 2012, 24, pp. 51-53, DOI: 10.1589/jpts.24.51.
[30] Kurz D., Dobrzycki A., Krawczak E., Jajczyk J., Mielczarek J., Woźniak W., Sąsiadek M., Orynycz O., Tucki K., Badzińska E. An Analysis of the Increase in Energy Efficiency of Photovoltaic Installations by Using Bifacial Modules. Energies 2025, 18, 1296, DOI: 10.3390/en18051296.
[31] Wieczorek B., Kukla M., Warguła Ł., Giedrowicz M., Rybarczyk D. Evaluation of Anti-Rollback Systems in Manual Wheelchairs: Muscular Activity and Upper Limb Kinematics during Propulsion. Sci. Rep. 2022, 12, 19061, DOI: 10.1038/s41598-022-21806-z.
[32] Borawski A., Mieczkowski G., Szpica D. Simulation Tests of Peripheral Friction Brake Used in Agricultural Machinery Shafts., May 20 2020.
[33] Brumercik F., Lukac M., Caban J., Krzysiak Z., Glowacz A. Comparison of Selected Parameters of a Planetary Gearbox with Involute and Convex-Concave Teeth Flank Profiles. Appl. Sci. 2020, 10, 1417, DOI: 10.3390/app10041417.